

Advancing AIE dipyrindyl derivative-based self-assembly system as robust probe with enhanced fluorescence by metal ion for sensing multiple solvents

Qingqing Wang, Huijuan Wu, Aiping Gao and Xinhua Cao*

College of Chemistry and Chemical Engineering, Green catalysis and synthesis key laboratory of Xinyang, Xinyang Normal University, Xinyang 464000, China. E-mail: caoxhchem@163.com.

Experimental

Reagents and materials

6-(dodecylcarbamoyl) picolinic acid was synthesized according to our previous work.⁴⁴ 6,6'-Diamino-2,2'-bipyridyl, 2,2'-Bipyridine-5,5'-diamine, 2,2'-Bipyridine-4,4'-diamine were purchased from Zhengzhou Alpha Chemical Co. LTD. Other reagents were purchased from Shanghai Darui Finechemical Co., Ltd. All other reagents are analytical grade.

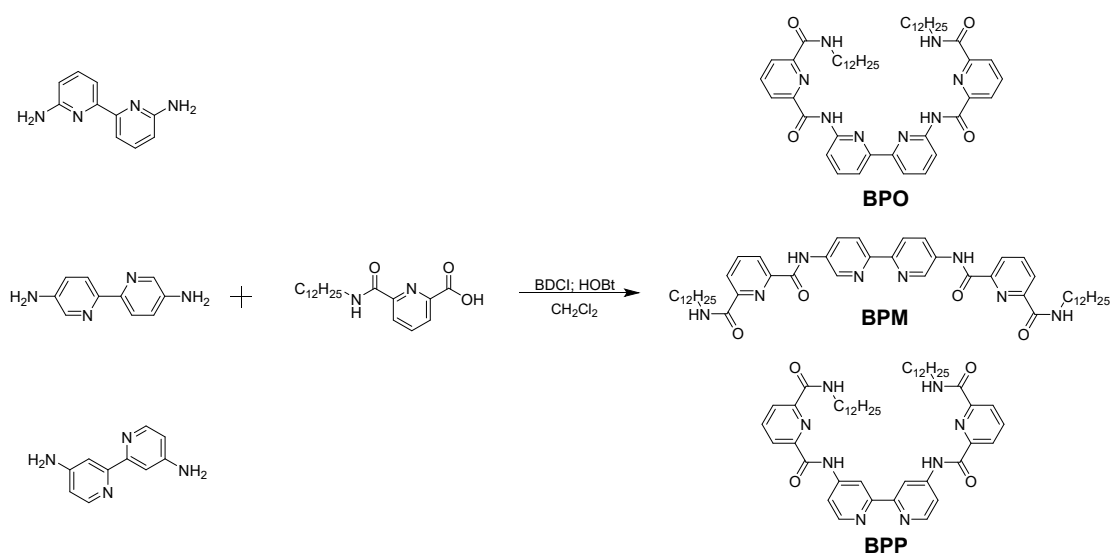
Characterization and instrumentations

¹H NMR and ¹³C NMR spectra were recorded in DMSO-*d*₆ on a 600 MHz and 150 MHz nuclear magnetic resonance spectrometer from Japan Electronics Co., LTD. (JNM-ECZ600R/S3). Proton chemical shifts were reported in parts per million downfield from tetramethylsilane. HRMS was recorded on a LTQ-Orbitrap mass spectrometer (ThermoFisher, San Jose, CA, USA). Field emission scanning electron microscope (FESEM) images were obtained using a FESEM S-4800 instrument (Hitachi, Ltd., Tokyo, Japan). Samples were prepared by spinning the samples on quartz plates and coating with Pt. Powder X-ray diffractions were generated by using a Philips PW3830 (Philips, Ltd., Eindhoven, Holland) with a power of 40 kV at 40 mA (Cu target, $\lambda = 0.1542$ nm). Fourier transform infrared (FTIR) spectra were collected by a Nexus470 spectrometer (Nicolet Company) with a resolution of 8 cm⁻¹, and 16 scans were accumulated to obtain an acceptable SNR. UV-vis absorption spectra were recorded on a UV-vis 3900 spectroscope (Hitachi, Ltd., Tokyo, Japan). Fluorescent spectra and fluorescence lifetime were recorded on an Edinburgh Instruments FLS 1000 (Edinburgh Instruments, Ltd. Livingston, UK). The absolute fluorescent quantum yields for samples were determined on an Edinburgh Instruments FLS 1000 absolute PL quantum yield spectrometer C11347 excited at 400 nm. Rheology experiments were performed on a MCR 301 Anton Paar (Austria) rheometer, with a Couette cell and a temperature control unit. The measurements were carried out on freshly prepared gels by using a controlled-stress rheometer. Parallel-plate geometry of 25 mm

diameter and 1 mm gap was employed throughout the dynamic oscillatory tests.

Gelation test

The gelation ability was tested via the inverse flow method reported in previous reference.



Scheme S1. The synthesis routines of **BPO**, **BPM** and **BPP**

Compound **BPO**, **BPM**, **BPP** were synthesized according to the synthesis routine in **Scheme S1**.

Synthesis of BPO: 6-(dodecylcarbonyl)picolinic acid (1.08g, 3.2mmol), 6,6'-Diamino-2,2'-bipyridyl (0.30g, 1.6mmol), EDCI (1.24g, 6.4mmol) and HOBt (0.44g, 3.2mmol) were mixed in CH₂Cl₂ (70 mL). The reaction mixture was stirred for 12 h at room temperature. After the reaction was over, the solvent was removed under reduced pressure and the residue was subjected to column chromatography (dichloromethane / methanol: 30/1, v/v as eluent) on silica gel to give **BPO** as a white powder. ¹H NMR (600 MHz, DMSO-*d*₆) δ 10.90 (s, 2H), 9.15 (s, 2H), 8.86 (s, 2H), 8.65 (d, *J* = 5.4 Hz, 2H), 8.32 (d, *J* = 7.7 Hz, 2H), 8.27 (d, *J* = 7.8 Hz, 2H), 8.21 (t, *J* = 7.7 Hz, 2H), 8.04 (m, *J* = 5.3 Hz, 2H), 3.42 (m, *J* = 6.7 Hz, 4H), 1.69 – 1.64 (m, 4H), 1.42 – 1.36 (m, 4H), 1.36 – 1.33 (m, 4H), 1.30 – 1.20 (m, 28H), 0.81 (t, *J* = 6.9 Hz, 6H). ¹³C NMR (150 MHz, DMSO-*d*₆): δ 163.57, 162.92, 154.60, 151.10, 150.47, 149.21, 139.61, 139.29, 125.56, 125.25, 117.92, 116.08, 31.77, 29.55, 28.89, 26.97, 21.60, 14.21. C₄₈H₆₆N₈O₄ [M+Na]⁺: 841.5105, found: 841.5137.

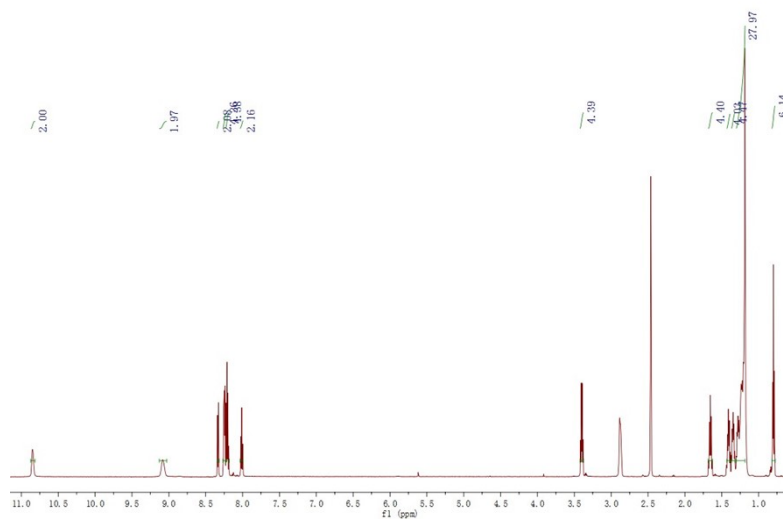


Fig. S1 The ^1H NMR spectra of BPO in $\text{DMSO-}d_6$.

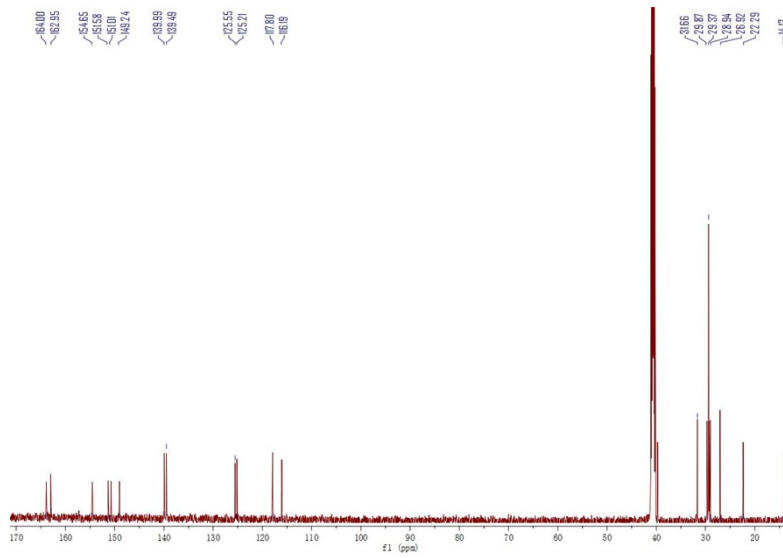


Fig. S2 The ^{13}C NMR spectra of BPO in $\text{DMSO-}d_6$.

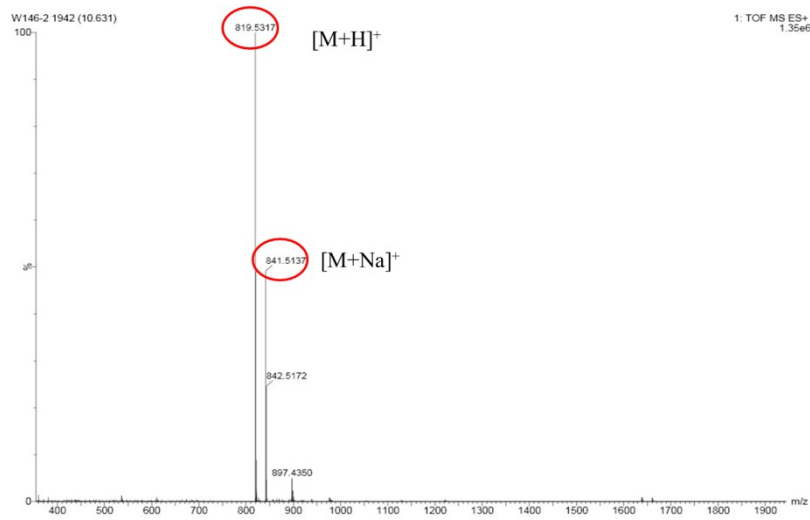


Fig. S3 The high resolution liquid chromatography spectra of **BPO**.

Synthesis of BPM: 6-(dodecylcarbonyl)picolinic acid (1.08g, 3.2mmol), 2,2'-Bipyridine-5,5'-diamine (0.30g, 1.6mmol), EDCI (1.24g, 6.4mmol) and HOBT (0.44g, 3.2mmol) were mixed in CH₂Cl₂ (70 mL). The reaction mixture was stirred for 12 h at room temperature. After the reaction was over, the solvent was removed under reduced pressure and the residue was subjected to column chromatography (dichloromethane / methanol: 30/1, v/v as eluent) on silica gel to give **BPM** as a white powder. ¹H NMR (600 MHz, DMSO-*d*₆): δ 10.89 (s, 2H), 9.22 (s, 2H), 9.12 (s, 2H), 8.43 (d, *J* = 8.5 Hz, 2H), 8.36 (d, *J* = 8.6 Hz, 2H), 8.32 (d, *J* = 7.6 Hz, 2H), 8.26 (d, *J* = 7.7 Hz, 2H), 8.21 (t, *J* = 7.7 Hz, 2H), 3.40 (m, *J* = 6.7 Hz, 4H), 1.66 – 1.60 (m, 4H), 1.37 (m, *J* = 5.2 Hz, 4H), 1.35 – 1.31 (m, 4H), 1.27 – 1.20 (m, 28H), 0.81 (t, *J* = 7.0 Hz, 6H). ¹³C NMR (150 MHz, DMSO-*d*₆): δ 163.78, 162.69, 151.67, 149.91, 148.40, 142.55, 139.76, 135.20, 129.58, 124.81, 120.73, 31.89, 29.30, 29.09, 26.71, 22.17, 14.39. C₄₈H₆₆N₈O₄ [M+H]⁺: 819.5285, found: 819.5245.

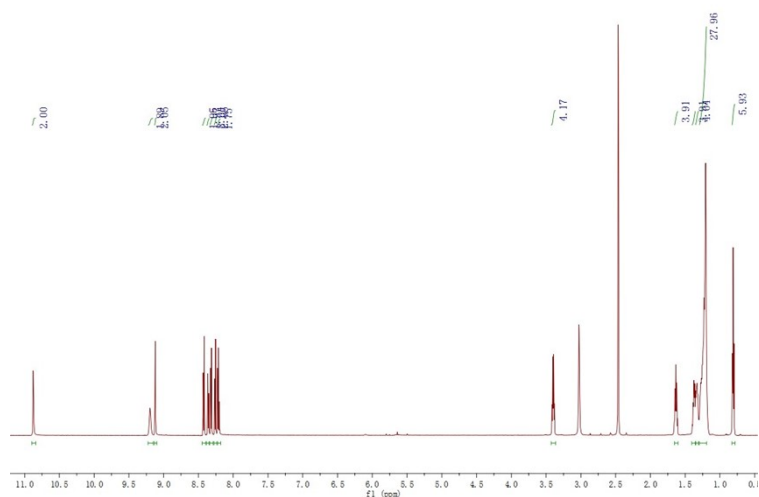


Fig. S4 The ¹H NMR spectra of **BPM** in DMSO-*d*₆.

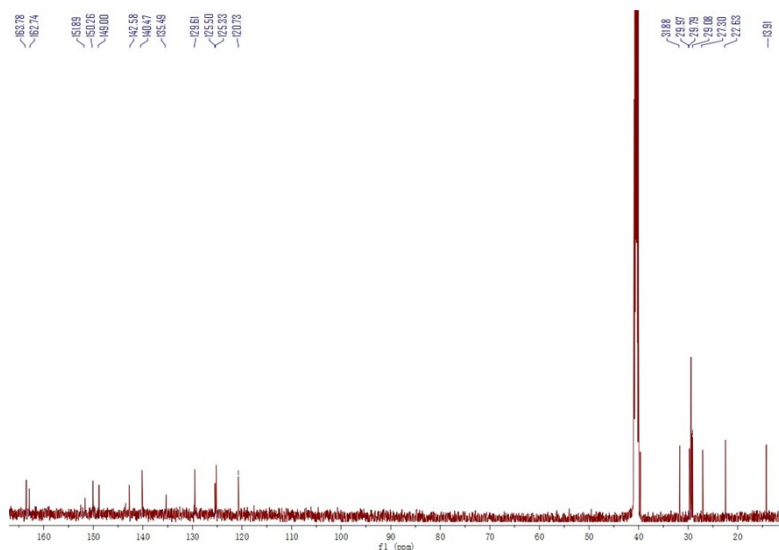


Fig. S5 The ^{13}C NMR spectra of **BPM** in $\text{DMSO-}d_6$.

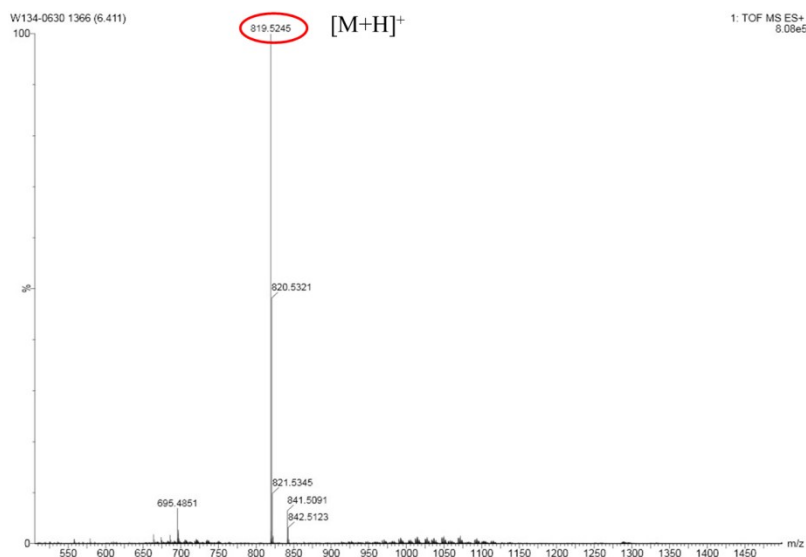


Fig. S6 The high resolution liquid chromatography spectra of **BPM**.

Synthesis of BPP: 6-(dodecylcarbonyl)picolinic acid (1.08g, 3.2mmol), 2,2'-Bipyridine-4,4'-diamine (0.30g, 1.6mmol), EDCI (1.24g, 6.4mmol) and HOBT (0.44g, 3.2mmol) were mixed in CH_2Cl_2 (70 mL). The reaction mixture was stirred for 12 h at room temperature. After the reaction was over, the solvent was removed under reduced pressure and the residue was subjected to column chromatography (dichloromethane / methanol: 30/1, v/v as eluent) on silica gel to give **BPP** as a white powder. ^1H NMR (600 MHz, $\text{DMSO-}d_6$) δ 10.90 (s, 2H), 9.15 (s, 2H), 8.86 (s, 2H), 8.65 (d, $J = 5.4$ Hz, 2H), 8.32 (d, $J = 7.7$ Hz, 2H), 8.27 (d, $J = 7.8$ Hz, 2H), 8.21 (t, $J = 7.7$ Hz, 2H), 8.04 (d, $J = 5.3, 1.9$ Hz, 2H), 3.42 (d, $J = 13.5, 6.7$ Hz, 4H), 1.69 – 1.63 (m, 4H), 1.43 – 1.37 (m, 4H), 1.34 (d, $J = 13.4, 6.5$ Hz, 4H), 1.30 – 1.20 (m, 28H), 0.81 (t, $J = 6.9$ Hz, 6H). ^{13}C NMR (150 MHz, $\text{DMSO-}d_6$): δ 163.58, 156.72, 150.88, 149.03, 146.85, 140.37, 125.58, 125.26, 115.67, 112.30, 31.71, 29.24, 28.67, 26.77, 22.44, 13.82. $\text{C}_{48}\text{H}_{66}\text{N}_8\text{O}_4$ $[\text{M}+\text{Na}]^+$: 841.5105, found: 841.5137.

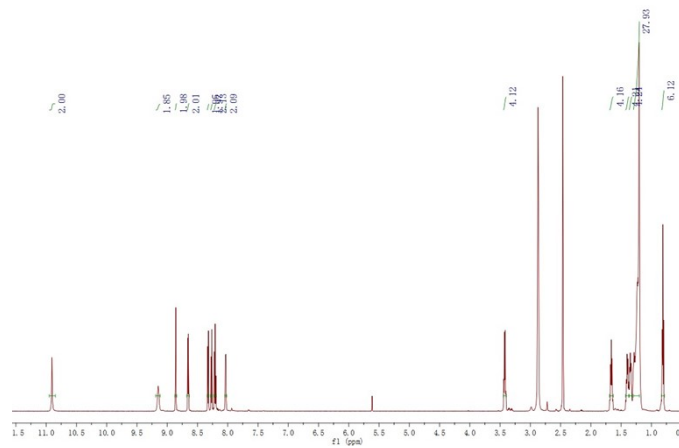


Fig. S7 The ^1H NMR spectra of BPP in $\text{DMSO-}d_6$.

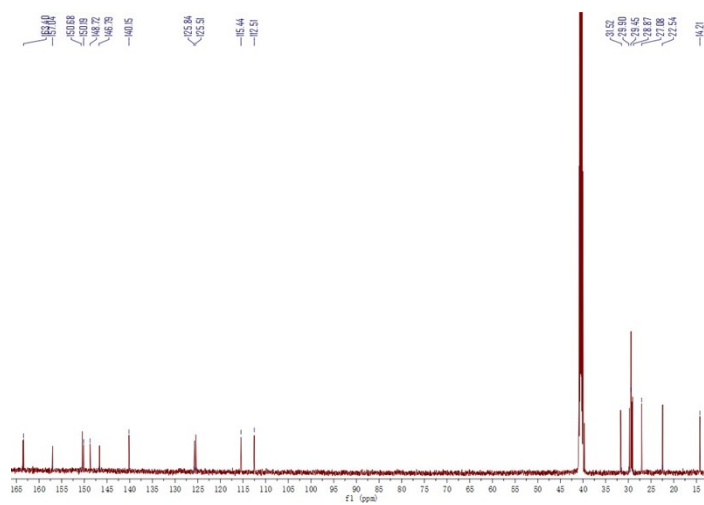


Fig. S8 The ^{13}C NMR spectra of BPP in $\text{DMSO-}d_6$.

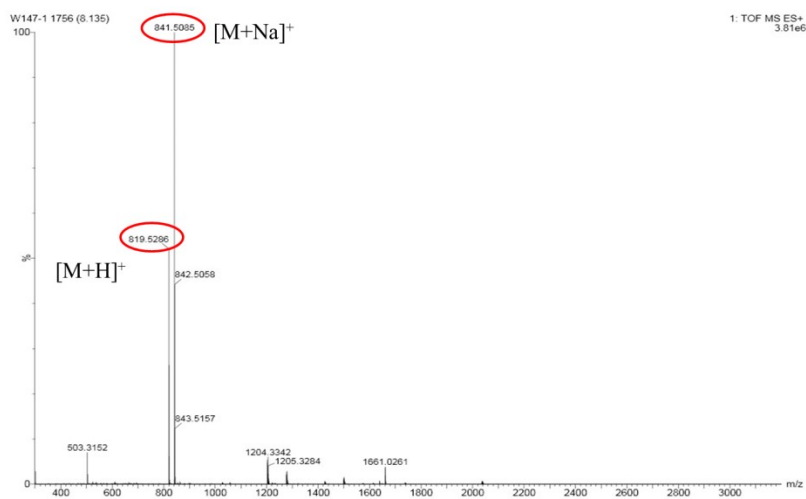


Fig. S9 The high resolution liquid chromatography spectra of BPP.

Table S1 T_{gel} of **BPO**, **BPM**, **BPP** in various solvents

sample	BPO				BPM	BPP
solvent	ethanol	acetone	DMSO	DMF	1,4-dioxane	toluene
$T_{gel} / ^\circ\text{C}$	90.2	90.2	90.2	80	42	100

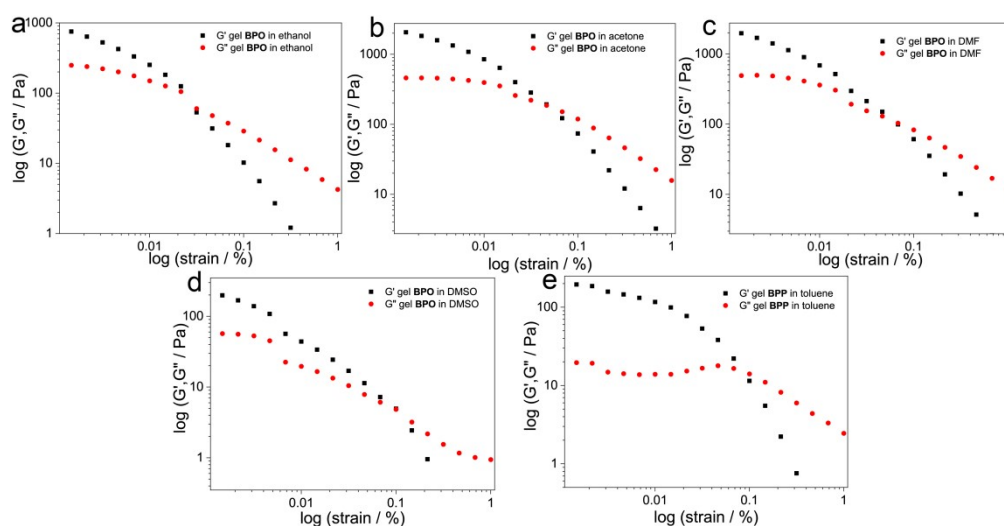


Fig. S10 Dynamic oscillatory data for gels of **BPO**, **BPM** and **BPP** in different solvents at their corresponding CGC at 20°C: (a) **BPO** for ethanol; (b) **BPO** for acetone; (c) **BPO** for DMF; (d) **BPO** for DMSO; (e) **BPM** for 1,4-dioxane; (f) **BPP** for toluene strain sweep of the gels at a frequency of 10 rad s⁻¹.

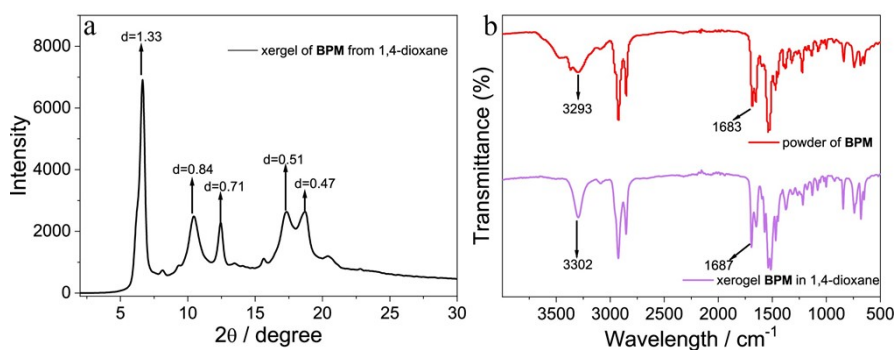


Fig. S11 (a) XRD patterns (b) FTIR spectra of powder **BPM** and xerogels **BPM** from 1,4-dioxane at their CGC.

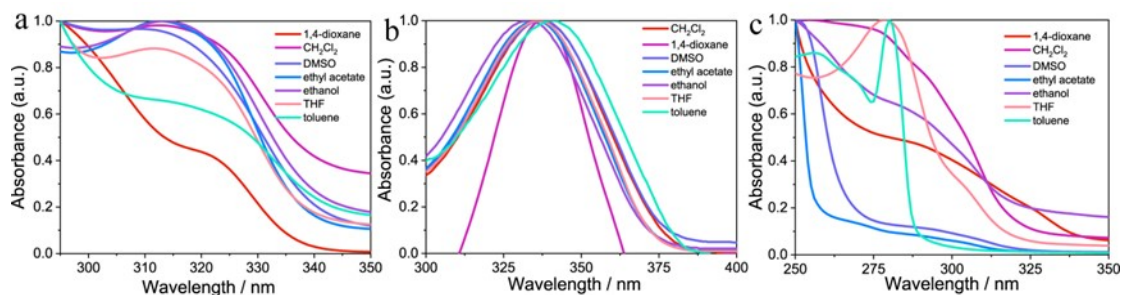


Fig. S12 UV-vis absorbance spectra of compounds (a) **BPO**, (b) **BPM** and (c) **BPP** in different solvent.

Table S2 Photophysical properties of **BPO**, **BPM**, **BPP** in various solvents

Solvents	BPO		BPM		BPP	
	$\lambda_{\text{abs,peak}}/\text{nm}$	$\lambda_{\text{PL,peak}}/\text{nm}$	$\lambda_{\text{abs,peak}}/\text{nm}$	$\lambda_{\text{PL,peak}}/\text{nm}$	$\lambda_{\text{abs,peak}}/\text{nm}$	$\lambda_{\text{PL,peak}}/\text{nm}$
1,4-dioxane	312	408	337	422	274	397
CH ₂ Cl ₂	310	/	337	422	260	/
DMSO	311	348	336	450	277	/
ethyl acetate	312	396	335	422	279	/
ethanol	314	395	332	422	300	/
THF	312	540	335	400	278	/
toluene	310	364	340	426	279	/

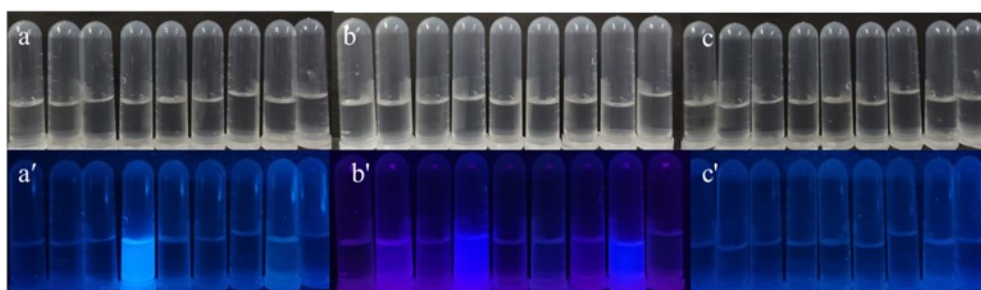


Fig. S13 Images of solutions **BPO**, **BPM** and **BPP** in different solvents; a and a' **BPO** for toluene, ethanol, acetone, 1,4-dioxane, DMSO, ethyl acetate, CH₂Cl, DMF, THF; b and b' **BPM** for DMSO, toluene, ethyl acetate, CH₂Cl₂, THF, 1,4-dioxane, DMF, ethanol, acetone; c and c' **BPP** for toluene, ethanol, acetone, 1,4-dioxane, DMSO, ethyl acetate, CH₂Cl₂, DMF, THF. The concentration of solution 1 was 10⁻⁵ M. The upper and lower were under daylight and 365 nm light, respectively.

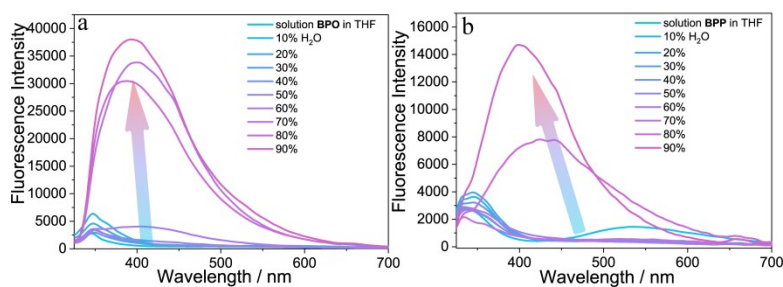


Fig. S14 Fluorescence spectra of solution **BPO** and **BPP** (10 μM) in the mixture solvents with different volume fractions (0-90%) of H₂O a) for **BPO** and b) for **BPP**. The excitation wavelengths are 315 nm

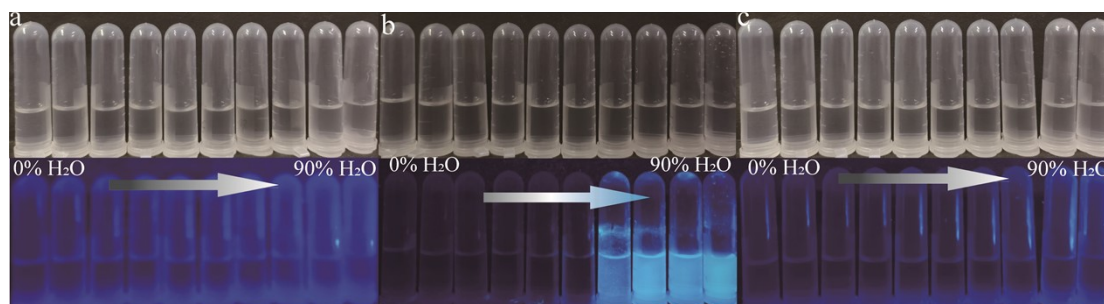


Fig. S15 Images solution **BPO**, **BPM** and **BPP** (10 μM) in the mixture solvents with different volume fractions (0-90%) of H₂O; a) for **BPO**; b) for **BPM**; c) for **BPP**.

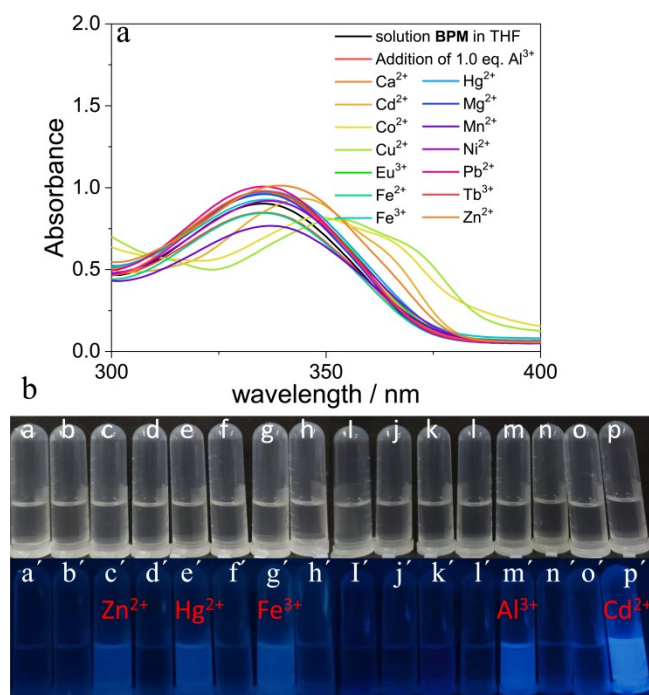


Fig. S16 (a) UV-vis absorption spectra change of solutions **BPM** in THF upon the addition of different metal ions; (a) images of (a) and a blank; b) Pb²⁺; c) Zn²⁺; d) Cu²⁺; e) Hg²⁺; f) Mn²⁺; g) Fe³⁺; h) Fe²⁺; i) Co²⁺; j) Ni²⁺; k) Eu³⁺; l) Tb³⁺; m) Al³⁺; n) Mg²⁺; o) Ca²⁺; p) Cd²⁺. The addition amount of different metal ions was 1.0 eq. The upper and lower were under daylight and 365 nm light, respectively. The concentration of solutions **BPM** was 10 μ M. The addition amount of different metal ions was 1.0 eq..

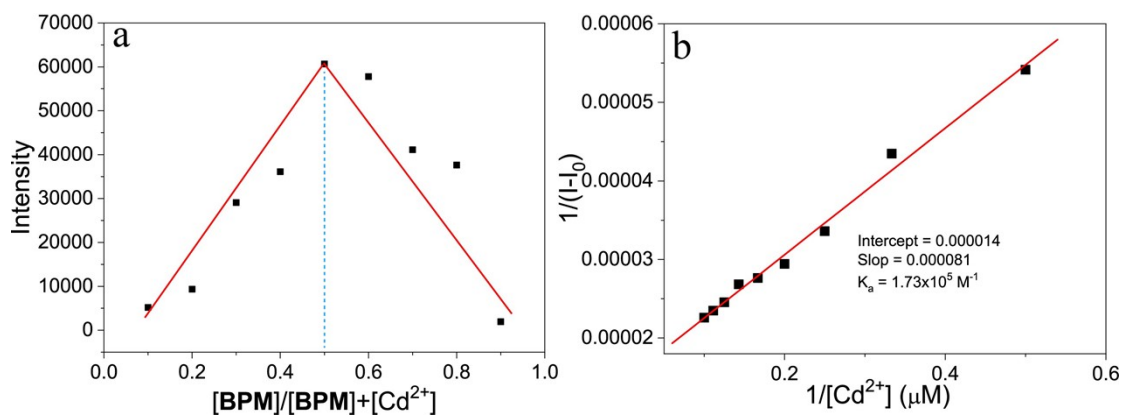


Fig. S17 (a) The Job plot showing the 1: 1 stoichiometry between Cd²⁺and **BPM**. (b) Benesi-Hildebrand plot. Fluorescence intensity at 400 nm.

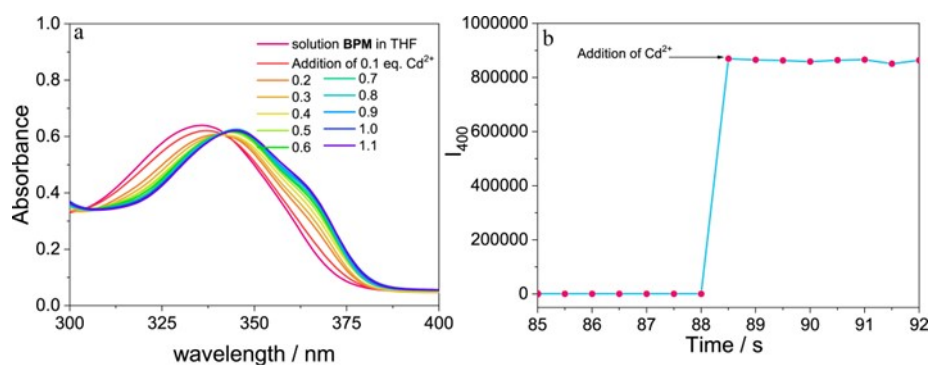


Fig. S18 (a) UV-vis absorption titration spectra of solution **BPM** in THF by Cd^{2+} ; (b) time-dependent fluorescence response of solution **BPM** to Cd^{2+} . The concentration of solutions **BPM** was $10\ \mu\text{M}$. The addition amount of different metal ions was 1.0 eq.

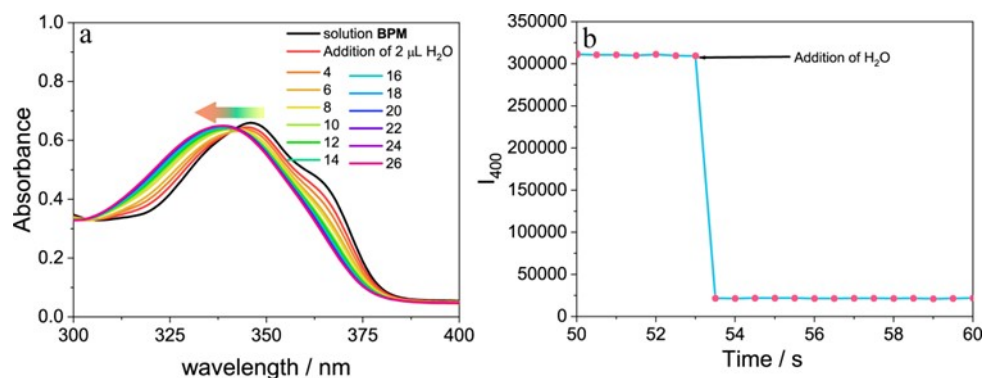


Fig. S19 (a) UV-vis absorption titration spectra of solution **BPM** in THF with 1.0 eq. Cd^{2+} by H_2O ; (b) time-dependent fluorescence response of solution **BPM-Cd** to H_2O . The concentration of solutions **BPM** was $10\ \mu\text{M}$. The addition amount of H_2O was $26\ \mu\text{L}$.

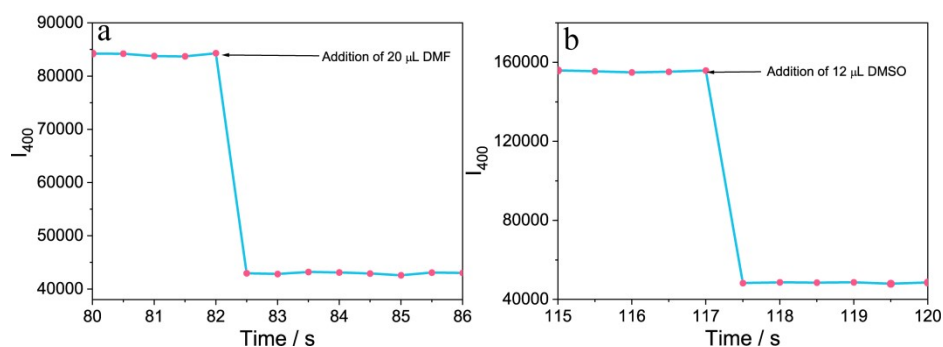


Fig. S20 Time-dependent fluorescence response of solution **BPM-Cd** to (a) DMF; (b) DMSO. The concentration of solutions **BPM** was $10\ \mu\text{M}$. The addition amount of DMF and DMSO were $24\ \mu\text{L}$ and $16\ \mu\text{L}$, respectively.

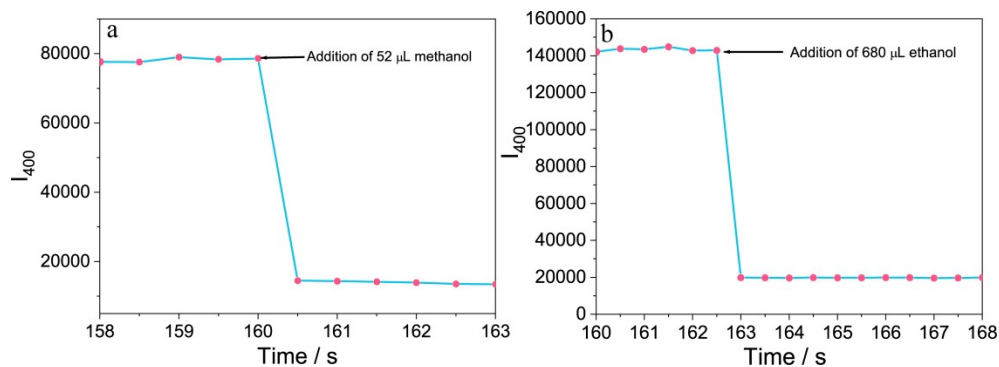


Fig. S21 Time-dependent fluorescence response of solution **BPM-Cd** to (a) methanol; (b) ethanol. The concentration of solutions **BPM** was $10\ \mu\text{M}$. The addition amount of methanol and ethanol were $52\ \mu\text{L}$ and $680\ \mu\text{L}$, respectively.

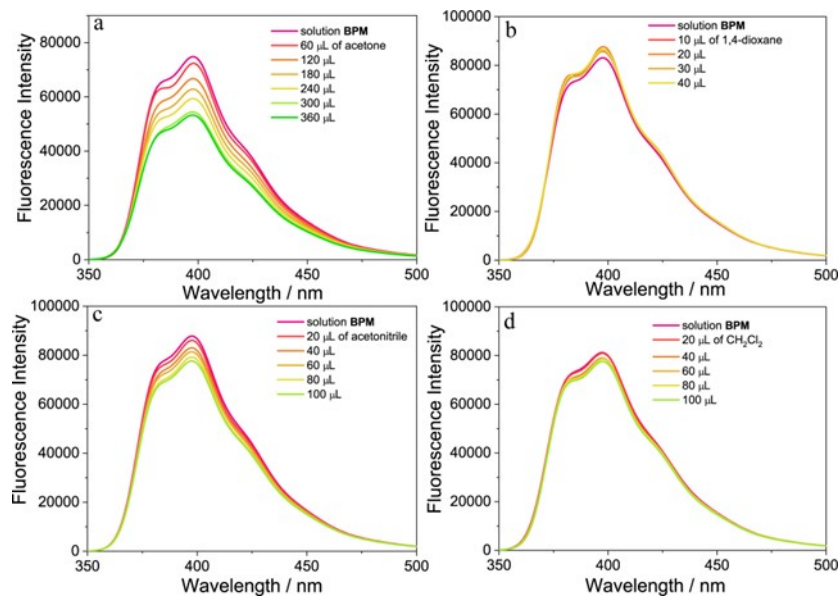


Fig. S22 Fluorescence spectra of solution **BPM** (10 μM) in THF with 1.0 eq Cd^{2+} under the titration of (a) acetone; (b) 1,4-dioxane; (c) acetonitrile (d) CH_2Cl_2 . The excitation wavelengths are 335 nm

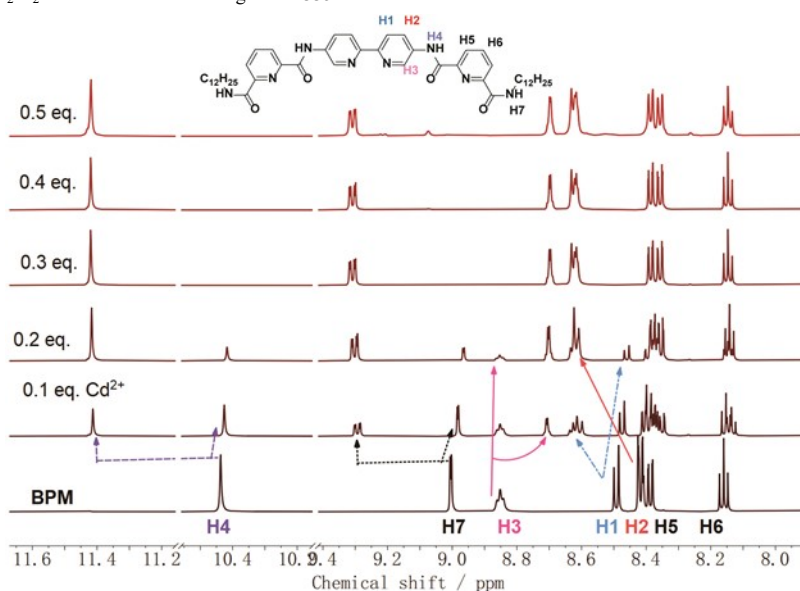


Fig. S23 ^1H NMR titration of solution **BPM** in $\text{THF-}d_8$ by Cd^{2+} .

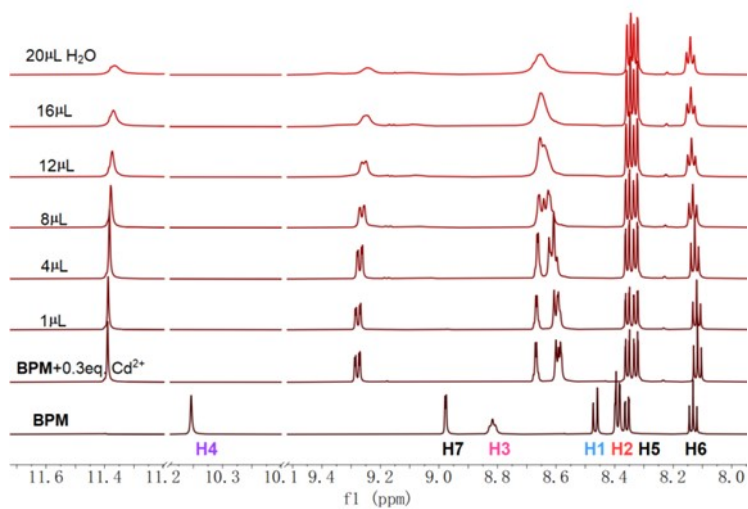


Fig. S24 ¹H NMR titration of solution **BPM-Cd** in THF-d₈ by H₂O.

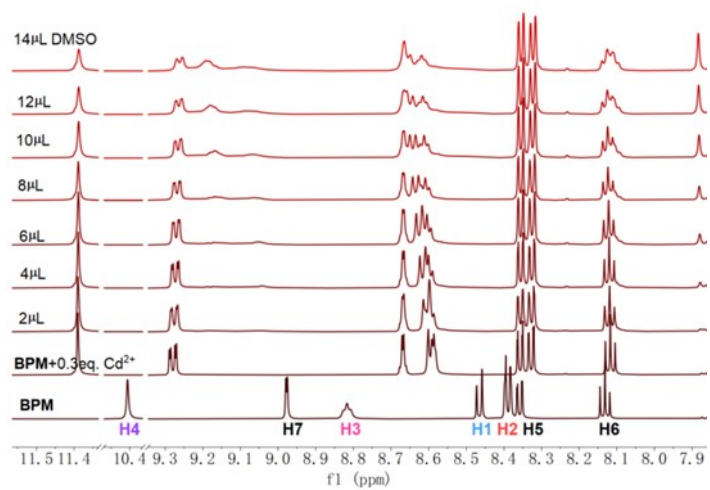


Fig. S25 ¹H NMR titration of solution **BPM-Cd** in THF-d₈ by DMSO.